Ion Channels, Transporters

Molecular cloning and functional characterization of the *Aplysia* FMRFamide-gated Na$^+$ channel

Yasuo Furukawa (✉) · Yoshiyuki Miyawaki · Genbu Abe

Y. Furukawa
Laboratory of Neurobiology, Faculty of Integrated Arts and Sciences, Hiroshima University, Kagamiyama 1-7-1, Higashi-Hiroshima 739-8521, Japan

Y. Miyawaki · G. Abe
Graduate School of Science, Department of Biological Science, Faculty of Science, Hiroshima University, Kagamiyama 1-3-1, Higashi-Hiroshima 739-8526, Japan

✉ Y. Furukawa
   Phone: +81-82-4246566
   Fax: +81-82-4240734
   E-mail: yasfuru@hiroshima-u.ac.jp

Abstract FMRFamide-gated Na$^+$ channel (FaNaC) is the only known peptide-gated ion channel, which belongs to the epithelial Na$^+$ channel/degenerin (ENaC/DEG) family. We have cloned a putative FaNaC from the *Aplysia kurodai* CNS library using PCR, and examined its characteristics in *Xenopus* oocytes. *A. kurodai* FaNaC (AkFaNaC) comprised with 653 amino acids, and the sequence predicts two putative membrane domains and a large extracellular domain as in other members of the ENaC/DEG family. In oocytes expressing AkFaNaC, FMRFamide evoked amiloride-sensitive Na$^+$ current. Different from the known FaNaCs (*Helix* and *Helisoma* FaNaCs), AkFaNaC was blocked by external Ca^{2+} but not by Mg^{2+}. Also, desensitization of the current was enhanced by Mg^{2+} but not by Ca^{2+}. The FMRFamide-gated current was depressed in both low and high pH. These results indicate that AkFaNaC is an FaNaC of *Aplysia*, and that the channel has *Aplysia* specific functional domains.

Keywords FMRFamide · Amiloride · ENaC · Ion channel · Cloning · *Aplysia*

Introduction

Neuropeptides are ubiquitous signaling molecules in the animal kingdom, and their structures are quite diverse. By contrast to the diversity of neuropeptides, almost all the known receptors for neuropeptides are G-protein coupled receptors. The FMRFamide-gated Na^+ channel (FaNaC) originally identified in *Helix* neurons [7, 8] is a rare exception [6]. FMRFamide directly activates Na^+ permeable ion channels that are blocked by amiloride [8, 14].

Molecular cloning of a cDNA encoding the FaNaC reveals that FaNaC is a member of the epithelial sodium channel/degenerin (ENaC/DEG) family [22]. The ENaC/DEG family is a unique class of ion channels having two transmembrane domains (M1 and M2), and the members show quite diverse functions [3, 21]: Na^+ absorption across tight epithelia (ENaC), mechanosensory transduction in nematodes (some of the degenerins), pain sensation following tissue acidosis [the acid-sensing ion channels (ASIC)], and peptidergic neurotransmission (FaNaC). FaNaC has been cloned from three species of molluscs (HaFaNaC from *Helix aspersa* [22]; HtFaNaC from *Helisoma trivolvis* [19]; LsFaNaC from *Lymnaea stagnalis* [26]). It is shown that four FaNaC subunits make the FaNaC [5].

Structure–function relationship of FaNaC has been studied using HaFaNaC and HtFaNaC. By the cystein-scanning mutagenesis, Poet et al. [28] have shown that N-terminal of M1 is involved in the conformation change for the channel opening, and that the selectivity filter is located in the outer vestibule of the channel. Based on the facts that the FMRFamide-sensitivity of HtFaNaC is 100 times less compared to HaFaNaC, and that HtFaNaC is rather potentiated by amiloride [19], a functional study using chimeric channels between HaFaNaC and HtFaNaC has identified a region involved in the FMRFamide recognition and the amiloride action [9]. As the latter study shows, the species-scanning mutagenesis can be a powerful strategy to reveal the functional domains of homologous proteins. For this strategy, the more the homologues are identified, the better. To better understand the structure-function relationship of FaNaC, we started to clone an *Aplysia* homologue of FaNaC. Here, we show molecular cloning and an initial functional characterization of *Aplysia kurodai* FaNaC (AkFaNaC) expressed in *Xenopus* oocytes.

Materials and methods

Molecular cloning

cDNA encoding a FaNaC of *A. kurodai* was obtained by PCR. An *A. kurodai* CNS cDNA library constructed in Uni-Zap (Stratagene, La Jolla, CA, USA) or a random-primed library of *A. kurodai* CNS constructed in λ-Zap (Stratagene) was used as a template for PCR. To design primers, we first examined the alignment of published cDNA sequences of FaNaCs from *H. aspersa* (X92113), *Helisoma trivolvis* (AF254118), and *L. stagnalis* (AF335548) by ClustalW [37]. Based on this information, we designed degenerate primers for nested PCR as follows: AAGAGRAARGTCATCTGGGC (S1), GGTCMGRAARTACCTSCAGTT (S2), GTASGYSCKGTCRTTGTTGAG (A1), ACHGAYTTSAGGTAGGACGT (A2). The first PCR (50 μl reaction) was carried out using the outer primer pairs (S1 and A1) and TaKaRa Taq DNA polymerase (TAKARA BIO Inc., Ootsu, Japan). PCR was performed as follows: 94°C 1 min, 68°C 7 min, 30 cycles. 3 μl of the first PCR product was used as a template for the second PCR by the inner primer pairs (S2 and A2). PCR cycles were identical to the first PCR. The nested PCR amplified several cDNAs including the one close to the expected size (≃960 bp). The amplified cDNA of ≃960 bp was gel-purified by GENECLEAN (Qbiogene, Irvine, CA, USA) and cloned into a T-vector, pGEM-Teasy (Promega, Madison, WI, USA). Four clones (T5 and T8 from the Uni-Zap library, R4 and R8 from the λ-Zap library) were partially sequenced by using Sequencing High (Toyobo, Osaka, Japan), and were confirmed to contain cDNAs corresponding to a middle part of AkFaNaC.

To obtain 5′ and 3′ ends of AkFaNaC, we designed gene specific primers of AkFaNaC based on the sequence information of the four clones described above. We first made two gene specific primers, ApFC-A2 (ACGGGTACTCCACGGGCATG) and ApFC-S2 (TCCGGACTGGAAGGATATAC). These primers were paired with the vector primers: uzp-S1 (ACCATGATTACGCCAAG) and T7-S (GTAATACGACTCACTATAGGGC). 5′ and 3′ rapid amplification of cDNA ends (RACE) were carried out using the primer pair uzp-s1//ApFC-A2 and the pair ApFC-S2//T7-S, respectively. The Uni-Zap library was used as a template. PCR, subcloning, and sequencing were done as described above. We obtained three clones containing 3′ end of AkFaNaC (#31,32,35), but 5′ RACE was not successful because of nonspecific amplification. To obtain 5′ end of AkFaNaC, we designed another gene specific primer downstream to ApFC-A2 (ApFC-A3, TGTTGCAGATGGTCACGGAC) and a vector primer downstream to

uzp-S1 (uzp-S2, AATTAACCCTCACTAAAG) for a nested PCR. The first PCR (25 μl reaction) for 5′ RACE was carried out using uzp-S1 and ApFC-A3. PCR was as follows: 94°C 1 min, 60°C 1 min, 72°C 1 min, 25 cycles. The second PCR was done using uzp-S2 and ApFC-A2. 0.5 μl of the first PCR product was used as a template, and the same PCR cycles were used. The second PCR products were subcloned as described. We obtained four clones containing 5′ end of AkFaNaC (#2–5). Multiple clones obtained by 5′ and 3′ RACE were sequenced, and a contig was compiled. Sequence information of AkFaNaC was deposited into GENBANK/EMBL/DDBJ database (Accession no. XXXXX)

Plasmid construction for cRNA synthesis

The coding region of AkFaNaC was amplified by two-step PCR. First, 5′ and 3′ regions that overlap each other were amplified using following primer pairs (sense//antisense): uzp-S1//ApFC-A1 (GCGGTCGTTGTTGAGCTGCT), ApFC-S1 (GGAAGTACCTGCAGTTCCAG)//T7-S. The Uni-Zap library was used as a template, and a high fidelity DNA polymerase, KOD DNA polymerase (Toyobo, Osaka, Japan), was used for amplification. PCR was as follows: 94°C 40 s, 60°C 40 s, 72°C 1.5 min, 25 cycles. PCR products were purified by GENECLEAN and dissolved into 30 μl TE. 0.5 μl of each PCR product was then mixed and used as a template for second PCR. The second PCR (50 μl reaction) was performed using ApFMRF-5S1 (CCTATGTTGGGTAGGGGTGAAAG) and ApFMRF-3A1 (CAGTCGTCATACGGGCGACTC). PCR cycles were the same to the first PCR. The amplified cDNAs were gel-purified, and cloned into a SmaI site of pBluescript II SK(+) (Stratagene). We sequenced both strands of two clones (#11, 17), and their sequences were confirmed to be identical to AkFaNaC. The EcoRI-XbaI fragments of the clones (#11, 17) were blunted, and cloned into the EcoRV site of pSD64TR, a modified vector originating from pSP64 (Promega, USA), to make pSD64TR-AkFaNaC. pSD64TR-AkFaNaC was linearized by XbaI, and cRNA was made by MEGAscript (Ambion, Austin, TX, USA).

Preparation of oocytes

Preparation of *Xenopus* oocytes and cRNA injection were essentially as described previously [27]. Briefly, a part of ovary was dissected out from an anesthetized frog in 0.15% tricaine. The ovary was treated with 2% collagenase (Type IA, Sigma, St Louis, MO, USA) dissolved in OR-2 medium (in mM: NaCl 82.5, KCl 2, $MgCl_2$ 1, HEPES 5, pH 7.5) at room temperature for 60~90 min. Dissociated oocytes were incubated at 18°C in ND96 (in mM: NaCl 96, KCl 2, $CaCl_2$ 1.8, $MgCl_2$

1, HEPES 5, pH 7.5) for 4~6 h before injection of cRNA. Oocytes of stage V–VI were selected and injected with 50 nl of cRNA containing solution. Injected oocytes were incubated for 2~4 days in ND96 supplemented with peniciline and streptomycine at 18°C before electrophysiological recording.

Electrophysiological recordings

Electrophysiological recording and data acquisition were essentially as described previously [36]. An oocyte was placed at the bottom of an experimental chamber ($\simeq$100 µl) and continuously perfused with ND96 ($\simeq$1 ml/min). The oocyte was impaled with two microelectrodes filled with a mixture of 3 M potassium acetate and 0.1 M potassium chloride (2–5 MΩ), and voltage-clamped by the oocyte clamp (Warner Instruments LLC., Hamden, CT, USA). Data were acquired by the Digidata 1200 and the Clampex (Ver. 6, Axon Instruments, Union City, CA, USA) and stored on the harddisk of an IBM-PC clone. In most experiments, a quashi-steady state membrane current was measured using a slow ramp command ($\simeq$90 mV/s). FMRFamide and drugs were applied via a small inlet tube placed close to the oocyte. Multiple reservers containing different solutions were connected to the inlet using fine tubings, and the solution was changed manually by switching a three-way valve connected at the bottom of each reserver. All the experiments were carried out at room temperature (20~25°C).

Data analysis

Digitized data were analyzed later by Clampfit (Axon Instruments) or Origin (Ver. 6, OriginLab Corporation, Northampton, MA, USA). Results of grouped data were expressed as means ± SE. The concentration–response relationship of the FMRFamide action was approximated by an equation,

$$I = I_{\max}\frac{A^n}{EC_{50}^n + A^n} \tag{1}$$

I and $I_{\max}$ are the amplitude of the FMRFamide-gated current and the expected maximum amplitude of the current, respectively. EC_{50} is the concentration of FMRFamide which evokes the half maximum response, [A] is a concentration of FMRFamide, and n is the Hill-coefficient. The Eq. 1 was also used to estimate parameters for the concentration-dependent blocking action of amiloride at micromolar range.

Amiloride block of AkFaNaC at micromolar range was found to be voltage-dependent, and the voltage-dependent dissociation constant ($K_D (V)$) was calculated assuming a one-to-one binding by a following equation,

$$\frac{I_{\mathrm{amiloride}}(V)}{I_{\mathrm{control}}(V)} = \frac{K_D(V)}{K_D(V) + [B]}$$

(2)

$I_{\mathrm{amiloride}}(V)$ and $I_{\mathrm{control}}(V)$ are the FMRFamide-gated currents in the presence and the absence of amiloride, respectively. $K_D(V)$ is the voltage-dependent dissociation constant, and $[B]$ is the concentration of amiloride.

The relationship between K_D and the membrane potential was fitted to an equation [40],

$$K_D(V) = K_D(0)\exp\left(\frac{z\delta V F}{RT}\right)$$

(3)

$K_D(0)$ is the dissociation constant at 0 mV, z is a valence of amiloride, and δ is a fraction of the electric field which is sensed by amiloride. F, R, and T have their usual meaning.

Solution and chemicals

Standard external solution was ND96 described above. Most chemicals were obtained from Katayama Chemical (Osaka, Japan). FMRFamide was purchased from Peptide Institute (Osaka, Japan). We also tested other known molluscan peptides or their analog peptides which contain –RFamide in their C-terminal structures. The tested peptides were FVRFamide (an analog of FMRFamide), LFRFamide (a truncated analog of the FRF peptides [10]), SDPFLRFamide [11], pQDPFLRFamide [29], and AdLGDHFFRFamide [12]. The peptides were generous gift from Dr. Fujisawa. The peptide was dissolved in ND96 as a concentrated stock (10^{-3} or 10^{-2} M), and kept in a freezer. The stock solution was diluted with appropriate experimental solution just before use. Reversal potentials of the FMRFamide-gated current were measured in 100 Na solution (in mM: NaCl 100, CaCl$_2$ 1.8, MgCl$_2$ 1, HEPES 5, pH 7.5) and 50 Na solution (in mM: NaCl 50, N-methyl-D-glucamine 50, CaCl$_2$ 1.8, MgCl$_2$ 1, HEPES 5, pH 7.5). To examine the effects of high divalent ions, 10 Ca solution (in mM: NaCl 85, CaCl$_2$ 10, HEPES 5) and 10 Mg solution (in mM: NaCl 85, MgCl$_2$ 10, HEPES 5) were used. Because NaCl was reduced in these high divalent solutions to keep the osmotic pressure, a control solution for such experiments was also modified as follows (in mM): NaCl 85, CaCl$_2$ 1.8, MgCl$_2$ 1, sucrose 21.6, HEPES 5. In some experiments, CaCl$_2$ in ND96 was replaced with MgCl$_2$ (2.8 Mg solution). To examine the effects of external

pH, pH of ND96 was changed to 8 or 6. When the acidic ND96 was made, HEPES in ND96 was replaced with MES. To test the blocking action of amiloride, amiloride (Sigma) was co-applied with FMRFamide. Amiloride containing solution was prepared just before use.

Results

Comparison of a primary structure of AkFaNaC with other molluscan FaNaCs

An open reading frame of AkFaNaC was 1959 base pairs and codes for a protein of 653 amino acids. As in other members of the ENaC/DEG family, two transmembrane regions (M1 and M2) and a large external domain were predicted by TMAP [31]. Figure 1 shows an alignment of amino acid sequences of AkFaNaC and other known molluscan FaNaCs. About 60% of amino acids are identical among different FaNaCs. Especially, two predicted transmembrane domains as well as their surrounding are well conserved. Because both M1 and M2 of the ENaC/DEG family are involved in the construction of the channel pore [4, 20, 28, 33, 35], almost identical sequences around M1 and M2 among FaNaCs suggest that FaNaCs have similar pore properties. The region between two transmembrane domains of AkFaNaC are cystein rich, and the number of cystein residues and their positions are almost completely identical in FaNaCs as noted by others [19, 22, 26], suggesting that the disulfide bonds in the external region are essential to determine the architecture of FaNaC. There are three putative PKC phosphorylation sites at N-terminal cytoplasmic domain, and two of them near M1 are well conserved in FaNaCs. Four out of eight putative *N*-linked glycocylation sites of AkFaNaC are also conserved in FaNaCs.

```
Aplysia   ...............MLGRGERIKPYHFRDSSADHMKYTSVAAKSGMVPEHR.YTMVRSRHHGRHHHHHSYQEYNTQRS   63
Helix     .......................................MKYTSAATKPGVFPEHHQHAMMRNRYHPHHCN......YSDNRS   38
Helisoma  .......................................MKYTGSEAKPSMSNSPHSYSSVKHRYQHTYSHS...DQESDGHT   41
Lymnaea   .....MYRSRVHSQNEAYARNGYISTRTRSETSSGHMKYTNIGSKPGMRPDQ..YSMGKPRGQPRH............T      60

Aplysia   AISLIAELGSESNAHGLAKIVTSRDTKRKVIWALMVIIGFTAATLQLSLLVRKYLQFQVVELSEIKDSMPVBYPSVTICN   143
Helix     AIDIIAELGSESNAHGLAKIVTSRDTKRKVIWALLVIAGFTAATLQLSLLVRKYLQFQVVELSEIKDSMPVQYPSVSICN   118
Helisoma  VLGIIAELGSESNAHGLAKIVTSRDTKRKVIWALLVIIGFTAATLQLSLLVRKYLQFQVVELSEIKDSMPVBYPSVTVCN   121
Lymnaea   ALGIIAELGSESNAHGLAKIVASHDTKRKVIWALLVIIGFTAATLQLSLLVRKYLQFQVVELSEIKDSMPVBYPSVTICN   140
                                            M1

Aplysia   IEPISLRKIRKAYNKNESQNLKDWLNFTQTFHFKDM.SFMNSIRAFYENLGTDAKKISHDLRDLLIHCRFNREECTTENF   222
Helix     IEPISLRTIRRMYFNNESQNLITWLRFIQKFRFEQD.SFMNSIRAFYENLGQDAKKLSHNLEDMLMHCRFNRELCHVSNF   197
Helisoma  IEPISITKILNLQNSTEGQKVINWLGFVTKFDFEQQKSFMDSFRAFYENLGDEAKMISHELADLLIHCRFNREICNLSNF   201
Lymnaea   TDPISLRKIRRSVFSNESLLLRSWLTFIETFKFEQS.AIMQSIRAFYENLGTEAKKISHDLQDLLIHCRFNREECSVSNF   219

Aplysia   TSSFDGNYFNCFTFNGGQLRDQLQMHATGPENGLSLIISIEKDEPLPGTYGVYNFENNILHSAGVRVVHAPGSMPSPVD   302
Helix     STFFDGNYFNCFTFNSGQR..LQMHATGPENGLSLIFSVEKDDPLPGTYGVYNFDNNILHSAGVRVVHAPGSMPSPVD   274
Helisoma  TTSFDGNYFNCFTFNGGQLADQLQMHATGPENGLSLIMSVEKAYPMPRFYGVYNFDNNILHSAGIRVVHAPGSMPSPVD   281
Lymnaea   TYSFDGNYFNCFTFNGGQLKEKLQMHATGPDNGLSLIISVEKDDPLPGTYGIYNFENNILHSAGIRVVHAPGSLPSPVD   299

Aplysia   HGFDIPPGYSSSVGLKALLHTRLSEPYGNCTEDSLEGIQTYRNTFFACLQLCKQRRLIRECKCKSSALPDLSVENITFCG   382
Helix     HGIDIPPGYSSSVGLKAILHTRLPYPYGNCTNDMLNGIKQYKYTFFACLQLCKQRLIIQRCGCKSSALPEVPSYNATFCG   354
Helisoma  HGIDIPPGYSSSVGLKALLHSRLPAPYGNCTMRSLQGMRTYRNTFFACLQLCKQRLIMSRCGCKSSALPDLPTENVTFCG   361
Lymnaea   QGIDIPPGYSSSVGLKALLHSRLSEPYGNCTEGTLQGMHTYRNTFFACLQLCKQNLIIRRCGCKSSALPDLPKENVTFCG   379

Aplysia   VIPDWKDIRRNVTGEYKMN.....QTIPTISLACEARVQKQLNNDRSYETDCGCYQPCSETSYLKSVSLSYWPLEFYQLS   457
Helix     VIKDWQEINRNHSNEDHNQSEEDRAFIPTPYLACEREQKNLNNDRTYELSCGCFQPCSETSYLKSVSLSYWPLEFYQLS   434
Helisoma  VIPNWEEIIKNVSGDVEPN.....MVIPTPALKCBERVQRELNNDRAYEMSCQCFQPCSETSYLKSVSLSYWPLEFYQQL   436
Lymnaea   VIPNWEKILRNESGDAFHG.....MTIPTPNLECBEKVHRELNNDRAYESECQCYQPCSETSYLKSVSLSYWPVEFYQLC   454

Aplysia   ALERFFSQKHPTDQQHFMKIAQDFLSRLAHPQQQALARNNSHDKDILTTSYSLSEKEMAKEASDLIRQNLLRLNIYLEDL   537
Helix     AVERFFKQERQAGQNHFMKTAYEYLEKLAHPSQKHLARNDSHMDDILSKSYSLSEKEMAKEASDLIRQNMLRLNIYLEDL   514
Helisoma  QLENILMTRNNTDKQHYMKKAYDILHTLSEEDRIRVMEKG.VD...VVPILMRRQKSLAKDASDMVRQNLIRLNIYLEDL   512
Lymnaea   VLQKFFN...ATDPDHFMKVAFYNLDKVAREGQAEMASDDNRK...FNKSYSDEQKKMTKEASDLIRQTMLRLNIYLEDL   528

Aplysia   SVVEYRQLPAYGLADLFADIGGTLGLWMGISVLTIMELMELIIRLFALIFNABEREVBKAPMHNSNNGGSGGGDGSGGQHN   617
Helix     SVVEYRQLPAYGLADLFADIGGTLGLWMGISVLTIMELIELVIRLTGLVFNSEKGLPRGPTTVNNNGSNNHSQSTSQHQ   594
Helisoma  SVVEYRQLPAYGLADLFADIGGTLGLWMGISVLTIMELVELIIRLIGLMFNVERKEPRAAVVPKKERAAPRRKSI.GHYP   591
Lymnaea   SVVEYRQLPAYGLADLFADIGGTLGLWMGISVLTIMELMELIIRLVGLVFS.ERDEPRRQTN.ETFTADNRRT....HPK   602
                                 M2

Aplysia   FANGDVEHERDTHFPD.LGSSDFDFRRGGGIGAESPV.   653
Helix     LYNGYMDHD..SHYSDSAGASVFDFRRG....VESPV.   625
Helisoma  TSNGDAKDV..TYYPDTYGPSEFDFRRT....AEAPV.   622
Lymnaea   TSN..APQE..SNYPDPFGAPEFNFRRG....VEAPPI   632
```

Fig. 1 Alignment of the FMRFamide-gated Na^+ channels. Two hypothetical transmembrane domains (M1 and M2) are predicted by TMAP. *Asterisk* shows conserved cysteins between M1 and M2. *N* indicates the hypothtical N-linked glycosylation sites. *Plus* indicates putative PKC phosphorylation sites. Although the N-terminal sequence of HtFaNaC may be longer as suggested by Perry et al. [26], we used the origical sequence by Jeziorski et al. [19] in this figure

## Functional expression of AkFaNaC in *Xenopus* oocytes

We examined electrophysiological properties of AkFaNaC in *Xenopus* oocytes under the two-electrode voltage-clamp. We first determined the concentration-response relationship for FMRFamide. Oocytes were voltage-clamped at -50 mV, and a known concentration of FMRFamide was applied by bath perfusion (30 s). FMRFamide evoked an inward current that shows modest desensitization (Fig. 2a). Even at the highest concentration tested (3×10^{-5} M), the current only

decayed to 74.6±2.1% of the peak current at the end of 30 s application of FMRFamide ($N=9$).

Figure 2b is an example of the concentration–response relationship from a single oocyte. Peak

amplitude of the FMRFamide-gated current was plotted against the concentration of FMRFamide,

and the relation was approximated by the Eq. 1. EC_{50} and the Hill coefficient (n) in this oocyte

were 3.7×10^{-6} M and 1.5, respectively. Mean EC_{50} and n of the concentration–response were

$3.8 \pm 0.2 \times 10^{-6}$ M and 1.60 ± 0.05, respectively ($N=5$). The Hill coefficient of more than one is also

reported in HaFaNaC [22, 41], and suggests a co-operativity for the channel opening [41].
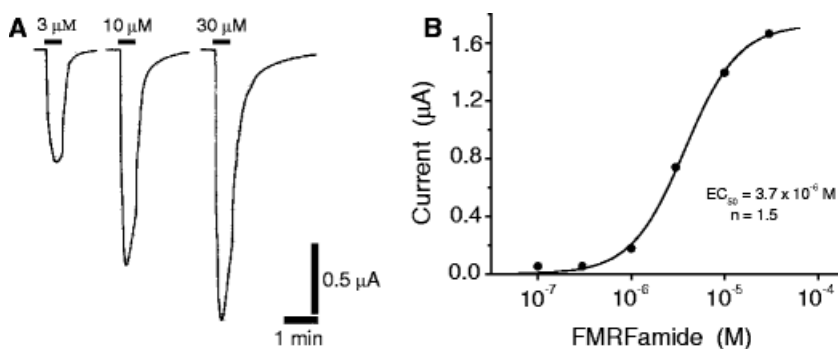
Fig. 2a–b AkFaNaC expresses the FMRFamide-gated Na$^+$ channels in *Xenopuse* oocytes. **a** The
FMRFamide-gated currents in an oocyte. Holding potential was −50 mV. FMRFamide was applied by
perfusion as indicated by bars. **b** The concentration–response relationship of the FMRFamide-gated current.
Peak amplitude of the FMRFamide-gated current is plotted against the concentration of FMRFamide. The
data was obtained from the same oocyte as shown in **a**. A smooth line is the best fit of the Eq. 1. EC_{50} and
n are 3.7×10^{-6} M and 1.5, respectively

There are numerous peptides having some similarity to FMRFamide in both invertebrate and

vertebrate nervous systems. To check the specificity of FMRFamide to AkFaNaC, we examined

some peptides having –RFamide in their C-terminal structures (see Materials and methods). Among

them, only FVRFamide had substantial action (Fig. 3). At the concentration of 10^{-4} M, the

FVRFamide-evoked current was 54.7±1.9% of the current evoked by 3×10^{-6} M FMRFamide

($N=6$). Thus, the agonistic action of FVRFamide is nearly 100 times less potent than that of

FMRFamide. Other peptides did not evoke measurable current at 10^{-4} M ($N=6$). These results are

consistent with the results obtained in HaFaNaC [6, 22], and suggest that FMRFamide is a specific

ligand for AkFaNaC.
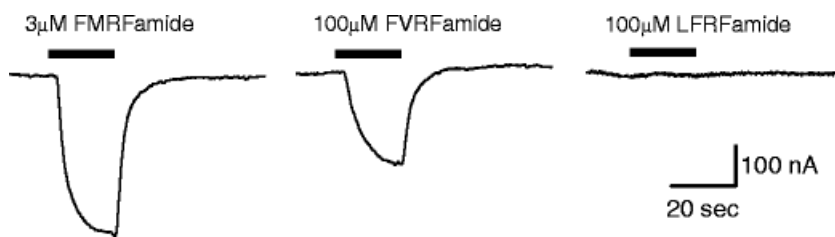
Fig. 3 Effect of some peptides having –RFamide in their C-terminal structure on AkFaNaC. Peptides were applied as indicated. Holding potential was −50 mV

We next determined the current–voltage (I–V) relationship of AkFaNaC. To this end, we used a slow voltage ramp because the FMRFamide-gated current shows little desensitization especially at lower FMRFamide concentration. A voltage ramp from −100 to +80 mV (≃90 mV/s) was applied every 10 s and 3×10^{-6} M FMRFamide was applied (Fig. 4a). Endogenous membrane currents in response to the voltage ramp (Fig. 4b1) were subtracted from the currents in the presence of FMRFamide (Fig. 4b2) to obtained the FMRFamide-gated current (Fig. 4c). The current between −100 and +80 mV in Fig. 4c corresponds to the *I–V* relationship of AkFaNaC. The *I–V* relationship of the FMRFamide-gated current showed clear inward rectification.
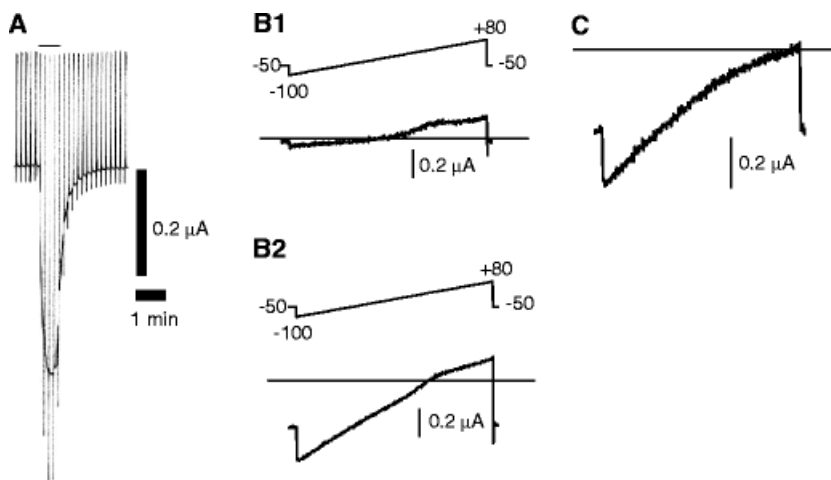
Fig. 4 Voltage-dependency of the FMRFamide-gated current. **a** The current evoked by 3×10^{-6} M FMRFamide (*bar*). *Vertical deflections* are the membrane currents evoked by ramp commands (from −100 to +80 mV, every 10 s). Holding potential was −50 mV. *Vertical bar* indicates 0.2 μA. **b** The membrane current in response to the ramp command in the absence (**b1**) or the presence (**b2**) of 3×10^{-6} M FMRFamide. The duration of the ramp was 1.92 s. The currents in **b1** and **b2** were obtained before and during the application of FMRFamide as shown in **a**. A *horizontal straight line* indicates the zero current level. **c** The FMRFamide-gated current isolated by subtraction. The current in the absence of FMRFamide (**b1**) was subtracted from the current obtained in the presence of FMRFamide (**b2**)

Figure 5 shows the I–V relationship of AkFaNaC in the solution containing either 100 mM (100 Na) or 50 mM (50 Na) NaCl. In 100 Na solution, the reversal potential (E_{rev}) of the FMRFamide-gated current was well beyond +50 mV. When external NaCl was reduced to 50 mM (50 Na), the E_{rev} was shifted to hyperpolarizing direction. Mean E_{rev} in 100 Na and 50 Na solutions were 64.3±2.0 mV and 45.8±2.1 mV, respectively (N=5). E_{rev} in 100 Na is well within the published values of the equilibrium potential of Na^+ in *Xenopus* oocytes [39]. In addition, the shift of E_{rev} is almost identical to the one expected from a perfect Na^+ electrode. Taken together, the results suggest that the AkFaNaC pore is selective to Na^+.
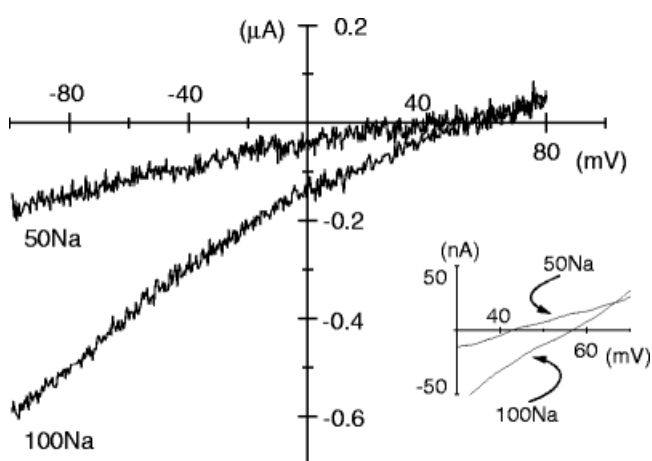

Fig. 5 Reversal potential of the FMRFamide-gated current. The FMRFamide-gated currents were obtained as described in Fig. 4 in 100 Na and 50 Na solutions, and presented as the current–voltage (I–V) relationship. The *inset* shows the higher magnification of the I–V relationships close to the reversal potentials. Smoothing of the currents was done by neighborhood averaging

Effect of amiloride on AkFaNaC

The channels in the ENaC/DEG family are usually blocked by amiloride [3, 21]. Amiloride blocks the FMRFamide-gated currents of HaFaNaC and LsFaNaC as well [8, 22, 26]. In contrast to a simple blockade of the current, the FMRFamide-gated currents of HtFaNaC were enhanced following the application of amiloride or related drugs [19]. In the single channel recording, the opening probability of HtFaNaC is shown to be increased by amiloride although the amplitude of single channel currents is depressed [19]. Therefor, in HtFaNaC, a balance between the potentiating and depressing actions of amiloride is shifted to the potentiation, resulting in the increase of the FMRFamide-gated current by amiloride [19].

In AkFaNaC, amiloride was seemed to block the channel simply as observed in most other members of the ENaC/DEG family at first sight. The concentration-response relationship, however, revealed some complex actions of amiloride. Figure 6 shows the actions of different concentrations of amiloride on AkFaNaC. Amiloride was co-applied with FMRFamide in this series of experiments. Even at 10^{-8} M, amiloride blocked substantial component of the FMRFamide-gated current (Fig. 6a). However, the blocking action of amiloride was clearly reduced at 10^{-7} and 10^{-6} M (see also Fig. 6c). The blocking action became stronger again at higher concentrations. Thus, there seems to be some potentiating action of amiloride on AkFaNaC that may be relevant to the result in HtFaNaC. The I–V relationship of AkFaNaC in 10^{-5} M amiloride indicated that the amiloride block at this concentration was voltage-dependent as often documented in ENaCs (Fig. 6b). Figure 6c shows the concentration-response relationships of the amiloride action in different membrane potentials. In $10^{-8} \sim 10^{-7}$ M, the voltage-dependency was rarely seen and the blocking action of amiloride was reduced by increasing the concentration of amiloride. At higher concentrations, clear voltage- and concentration-dependent blocking became obvious. When the concentration–response relationship in a higher concentration range ($10^{-6} \sim 10^{-4}$ M) was fitted with the equation (1), the absolute value of n was close to 1 (0.9~1.1) if the membrane potential was < -30 mV (not shown), suggesting that amiloride blocks AkFaNaC by a one-to-one binding. At higher membrane potentials, n became much larger than 1. The reason is not immediately clear but it might be due to the relative increase of the potentiating action of amiloride.


12
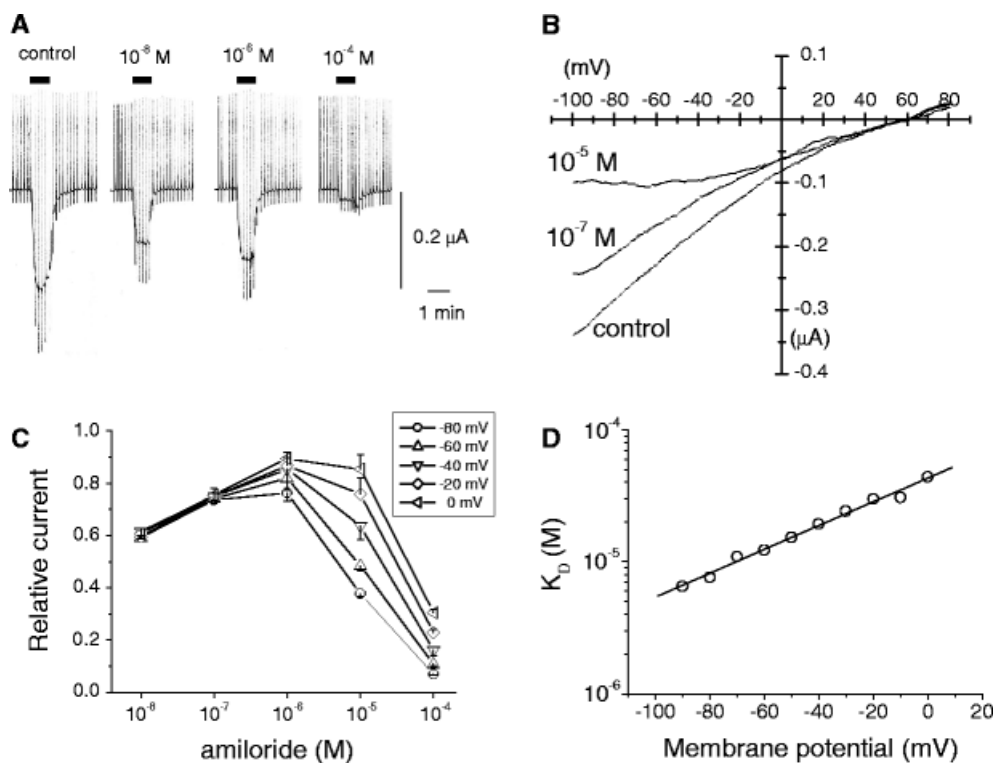
Fig. 6 Actions of amiloride on the FMRFamide-gated current. **a** Examples of the amiloride action on the FMRFamide-gated current. The FMRFamide-gated currents were evoked by 3×10^{-6} M FMRFamide (*bars*). Amiloride (the concentration is shown above each trace) was co-applied with 3×10^{-6} M FMRFamide. **b** The I–V relationships of the FMRFamide-gated current in the absence (control) or the presence (10^{-7} or 10^{-5} M) of amiloride. **c** The concentration–response relationships of the amiloride actions obtained at different membrane potentials. The currents at different membrane potentials were obtained from the I–V relationship as shown in B, and the current in the presence of amiloride was divided by the control current. The mean $\pm$ SE of the relative current (*N*=3) is plotted against the concentration of amiloride. Note the concentration–response relationship is ∩-shape, indicating the mixed action of amiloride (inhibition and potentiation). **d** Voltage-dependency of the dissociation constant (K_D) of amiloride. K_D was estimated by the Eq. 2 using the data obtained in 10^{-4} M amiloride, and plotted against the membrane potential. Smooth line was fitted by the Eq. 3. $K_D(0)$ and δ were estimated to be 4.3×10^{-5} M and 0.53, respectively

We analyzed the voltage-dependent block of AkFaNaC by amiloride in the higher concentration range using the Woodhull model [15, 40]. We assumed a one-to-one binding of amiloride with AkFaNaC. Based on the data obtained for 10^{-4} M amiloride, the dissociation constants (K_D) of the blocking action in different membrane potentials were calculated using the equation (2). Estimated $K_D(V)$ was plotted against the membrane potential, and fitted with the equation (3) (Fig. 6d). *z* of amiloride was assumed to be one [17, 23, 24, 34]. $K_D(0)$ and δ were estimated to be 4.3×10^{-5} M and 0.53, respectively. The results suggest that amiloride occludes the ion permeation pathway of AkFaNaC by binding a site sensing about 50% of the electric field from the outside.

Effect of divalent ions on AkFaNaC

In HaFaNaC and HtFaNaC, external Ca^{2+} and Mg^{2+} are known to block the channels at their physiological concentration range (less than a few mM). As in other marine invertebrates, the ionic composition of *Aplysia* hemolymph is supposed to be close to that of the sea water which contains ~10 mM Ca^{2+} and 50–60 mM Mg^{2+}. Indeed, it is reported that the hemolymph of some *Aplysia* contains 13.3 mM Ca^{2+} and 49 mM Mg^{2+} [30]. So, we next examined the effect of high Ca^{2+} or Mg^{2+} containing solution on AkFaNaC. When external solution was changed to the one containing 10 mM Ca^{2+} and no Mg^{2+} (10 Ca), the FMRFamide-gated current was much reduced (Fig. 7a1, b). As seen in Fig. 7a1, the Ca^{2+} block was mostly voltage-independent. By contrast to the blocking action of Ca^{2+}, the FMRFamide-gated current was greatly enhanced if the external solution contains 10 mM Mg^{2+} and no Ca^{2+} (10 Mg). Apparent potentiating action of Mg^{2+} is presumably due to the removal of the Ca^{2+} block because still larger current was observed in a

nominally Ca^{2+} free solution (2.8 Mg, Fig. 7b). These results suggest that external Ca^{2+} but not Mg^{2+} has a potent blocking action on AkFaNaC. Mg^{2+} seems to have much weaker blocking action (compare the result in 10 Mg and 2.8 Mg in Fig. 7b).
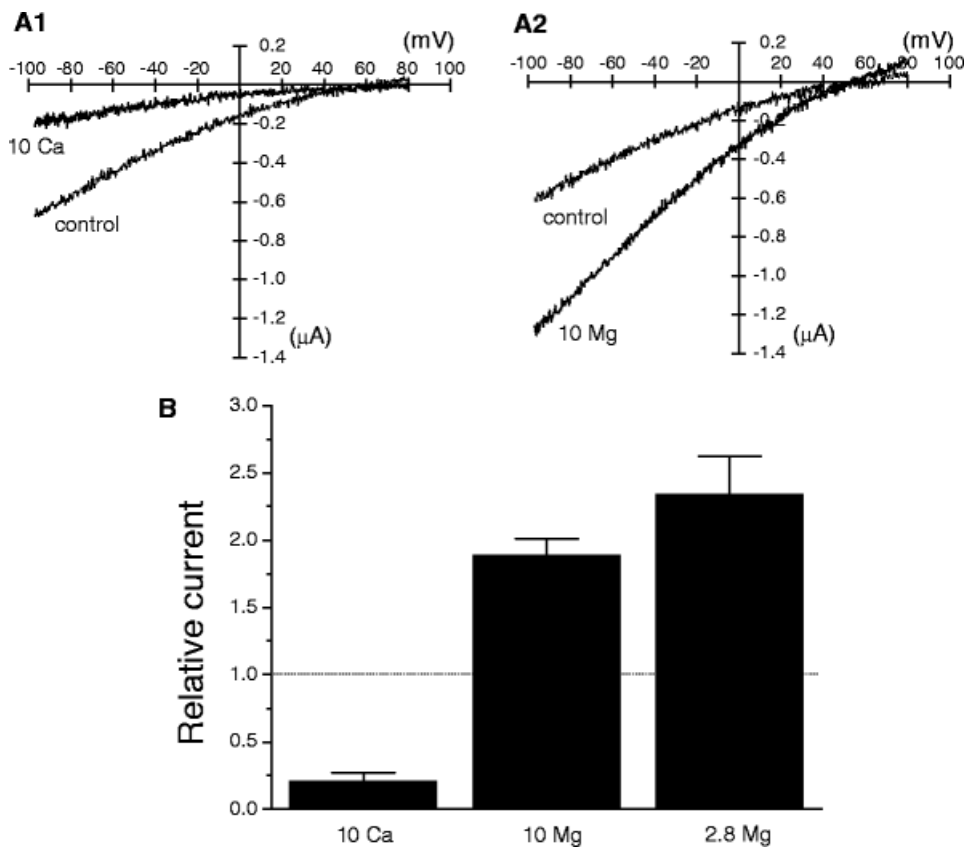
Fig. 7 Effects of external Ca^{2+} and Mg^{2+} on the FMRFamide-gated current. **a** The I–V relationship in 10 Ca (**a1**) and 10 Mg (**a2**). The I–V relationships were obtained as described in Fig. 4. The control I–V was obtained in 85 Na solution containing 1.8 mM Ca^{2+} and 1 mM Mg^{2+} (see Materials and methods). **a1** and **a2** were obtained from the same oocyte. **b** Comparison of the amplitude of the FMRFamide-gated currents in different divalent conditions. The relative currents at −80 mV were calculated by dividing the currents in high divalent conditions with the control currents. *Histogram* shows the mean value of the relative currents, and the *error bar* indicates SE of the mean (*N*=5)

As noted earlier, AkFaNaC shows little desensitization in response to μM range of FMRFamide in ND96. The desensitization was found to be modified by external divalent ions. Figure 8 compares FMRFamide-gated currents at −50 mV in response to one minute application of 3×10^{-6} M FMRFamide in different ionic conditions. In the control solution containing 1.8 mM Ca^{2+} and 1 mM Mg^{2+}, a little desensitization was observed (Fig. 8a). In 10 Ca, no desensitization was observed but a sluggish increase of the current was seen (Fig. 8b). By a sharp contrast, marked desensitization became apparent in 10 Mg. The results were confirmed in three other oocytes.
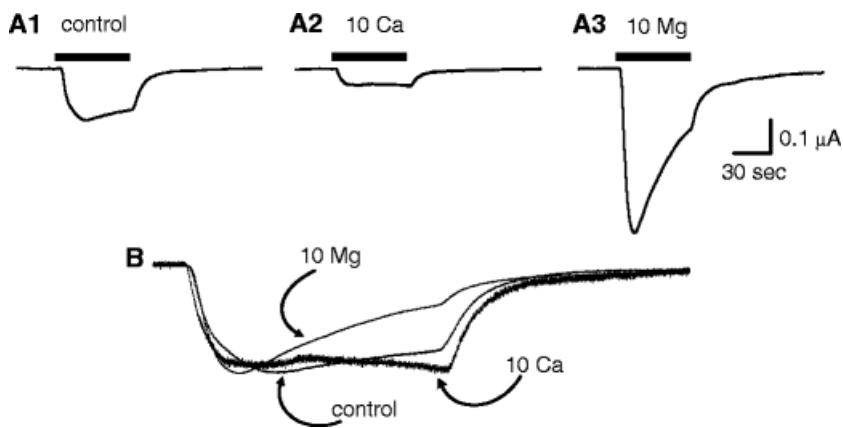
Fig. 8 External divalent ions affect the desensitization of the FMRFamide-gated current. **a** The FMRFamide-gated current in control (**a1**), 10 Ca (**a2**), or 10 Mg (**a3**). Holding potential was −50 mV. 3×10^{-6} M FMRFamide was applied for one minute as indicated by *bars*. **b** Comparison of the time course of the FMRFamide-gated currents. The currents shown in **a** are superimposed after adjusting their amplitudes appropriately

Effect of external pH on AkFaNaC

Perry et al. [26] investigated the FMRFamide-gated current in a *L. stagnalis* neuron which expresses LsFaNaC. They found that the FMRFamide-gated current is blocked at both acidic and alkaline pH. Moreover, the endogenous FMRFamide-gated current in the *Lymnaea* neuron shows less desensitization in acidic solution. We therefor examined the effects of acidic and alkaline ND96 on AkFaNaC (Fig. 9). pH of the control ND96 was 7.3 in this experiment. In the tested pH range (pH 6–8), the membrane currents in response to a voltage ramp (−100 to +80 mV) was little affected in the absence of FMRFamide. The FMRFamide-gated current was depressed in both acidic (pH 6) and alkaline (pH 8) ND96 as observed in the *Lymnaea* neuron (Fig. 9). In either case, little voltage-dependency is found for the blocking actions. Depression of the FMRFamide-gated current in pH 6 (<20% of the control) was much larger compared to FMRFamide-gated current in the *Lymnaea* neuron at the same pH (≃74% of the control [26]). As noted above, the desensitization of AkFaNaC is modest in the normal ND96. We did not observe noticeable change of the desensitization of AkFaNaC in either acidic or alkaline ND96 examined in the present study.
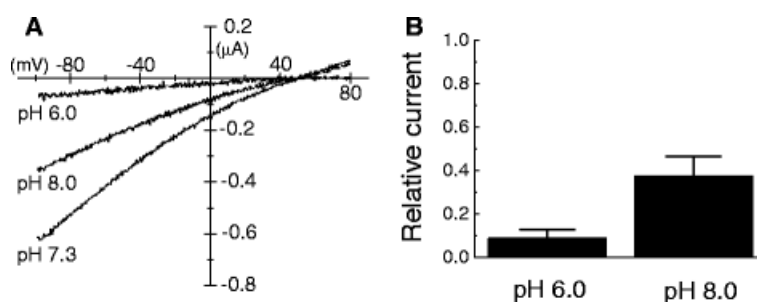
Fig. 9 Effects of external pH on the FMRFamide-gated current. **a** The I–V relationships of the FMRFamide-gated currents in different pH. The I–V relationships were obtained as described in Fig. 4. **b** Blockade of the FMRFamide-gated currents in acidic and alkaline pH. The relative currents at −80 mV in pH 6.0 or pH 8.0 were calculated by dividing the corresponding currents with the current in pH 7.3. Histogram shows the mean value of the relative currents, and the error bar indicates SE of the mean (N=7 for pH 6.0, N=6 for pH 8.0)

Discussion

We have cloned an *A. kurodai* homologue of the FMRFamide-gated Na^+ channel (AkFaNaC). AkFaNaC comprises with 653 amino acids and about 60% identical to other known molluscan FaNaC (HaFaNaC, HtFaNaC, and LsFaNaC). Application of FMRFamide to *Xenopus* oocytes expressing AkFaNaC evoked the amiloride-sensitive Na^+ current. The EC_{50} and the Hill coefficient were around 4×10^{-6} M and 1.6, respectively. These values are close to the ones reported in HaFaNaC [22]. Although FMRFamide is known to activate the Na^+ currents in some *Aplysia* neurons [2, 32], the molecular entities of the channels are not yet established. Present study shows that *Aplysia* also express FaNaC in its nervous system, and suggests that FMRFamide-activated Na^+ currents documented in some *Aplysia* neurons are flowing through the channels constructed with *Aplysia* FaNaC. The FMRFamide-activated Na^+ currents in *Aplysia* shows much faster desensitization compared to the FMRFamide-gated Na^+ current of AkFaNaC in oocytes. Similar functional difference of the FMRFamide-gated currents between cloned and endogenous channels is also reported in *Helix* and *Helisoma* channels [6, 19]. Because high Mg^{2+} was found to enhance the desensitization of AkFaNaC, some of the difference between the *Aplysia* neuronal FMRFamide-gated current and the AkFaNaC current in oocytes may be due to the different composition of the physiological saline (the artificial sea water for *Aplysia* neurons vs ND96 for frog oocytes).

FaNaC is a member of the ENaC/DEG family [3, 21]. The ENaC/DEG family channels contain two transmembrane domains (M1 and M2) and a large external domain that is cystein-rich. The position of many cystein residues is well conserved, suggesting that intramolecular disulfide bonds are necessary to make three dimensional structure of the external domain [21]. Mutagenesis studies in ENaC [33] have identified the selectivity filter and the binding site of a pore blocker, amiloride, in the pre-M2 and N-terminal of M2 (the pore region). The substituted cystein-accessibility study in the pore region suggest that the region also participates in the gating of ENaC [35]. The M1 region is also involved in the channel gating [38] and the ion conduction pathway [28]. Because the region is well conserved among the family members [21], the pore structure of the ENaC/DEG family channels is supposed to be similar.

As in other members in the ENaC/DEG family, AkFaNaC was blocked by amiloride but the amiloride action was found to be complex. Although the concentration lower than 10^{-8} M was not tested in the present study, AkFaNaC is apparently blocked by a nanomolar range of amiloride (see Fig. 6). The blocking action at such lower concentration range was not noticeably voltage-dependent, but the blocking action at micromolar range was clearly voltage-dependent. These results are explainable if we assume at least two distinct binding sites for amiloride in AkFaNaC. In ENaC, two positions in the primary structure are identified to be involved in the binding of amiloride: the one is in the external loop and the other is in the ion permeation pathway [18, 33]. These two sites may not necessarily be distant from each other in the three dimensional structure [18]. The binding site in the permeation pathway is consistent with a voltage-dependency of the amiloride block in ENaC [17, 23, 24, 34]. Published values of δ for the amiloride block of ENaCs are mostly in a range of 0.1~0.2 (but see [34]). Based on the voltage-dependent K_D for the amiloride block in the micromolar range, δ was estimated to be ≃0.5 in AkFaNaC, suggesting that amiloride occludes the ion permeation pathway of FaNaC. Our result is consistent with the result of single channel recording of HtFaNaC [19], in which amiloride depresses the amplitude of the single channel current, suggesting a fast open channel blockade by amiloride [15]. Although our estimation of $K_D(V)$ is likely to be contaminated by multiple actions of amiloride, estimated δ is much larger than the estimated values in ENaCs, suggesting that the pore structure of FaNaC may be substantially different from that of ENaC.

In the present study, a reduction of the amiloride block was clearly observed in some concentration range, suggesting that amiloride can also modify the channel function in addition to the pore block. In HtFaNaC, the overall action of amiloride is the potentiation of the FMRFamide-gated current because of its enhancing action of the channel open probability [19].

Similar enhancement of the open probability has been described recently in the neuronal FMRFamide-gated channels of *Helix* [13]. These observations suggest that the amiloride binding at not yet identified site(s) of FaNaC may allosterically modify the channel gating. Although amiloride is usually categorized as a blocker of the ENaC/DEG family channels, a potentiating action of amiloride and related drugs may not be unique to FaNaC. In some mutant of BNC1 (also called MDEG or BNaC1) which is a member of the ENaC/DEG family, amiloride can activate the current through the channel [1].

Based on the single channel recording, both HaFaNaC and HtFaNaCs as well as the endogenous FMRFamide-gated channels of the *Helix* and *Helisoma* neurons are shown to be blocked by submillimolar Ca^{2+} or Mg^{2+} [13, 19]. These divalent ions induce a flickering block of the open FaNaC at similar concentration, which apparently reduces the amplitude of single channel currents [13, 19]. Although the flickering block and the reduced single channel current suggest the fast open channel blockade [15], the divalent ion block in *Helix* neuronal FMRFamide-gated channels lacks a clear voltage-dependency [13]. In AkFaNaC, Ca^{2+} but not Mg^{2+} can reduce the FMRFamide-gated current, suggesting that the binding site is more specific compared to the divalent blocking site suggested in other FaNaCs. Because the Ca^{2+} block in AkFaNaC was not voltage-dependent, the binding site is presumably outside of the membrane electric field. Thus, AkFaNaC seems to have a divalent blocking site that is functionally different from HaFaNaC or HtFaNaC. The voltage-independent Ca^{2+} block in AkFaNaC as well as in other FaNaCs might be related to a weakly voltage-dependent Ca^{2+} block in ASIC (δ=0.054 in ASIC1b, [25]). ASIC is an acid-sensing channel that is activated by H^+. Recently, Immke and McCleskey [16] have suggested that the opening of ASIC by H^+ is actually a relief of the Ca^{2+} block by multiple H^+ binding. Moiety for the Ca^{2+} block in FaNaC would be, however, different from that of ASIC, because external H^+ rather blocked the FMRFamide-gated current of AkFaNaC (this study) as well as the neuronal FMRFamide-gated current of *Lymnaea* [26]. Modification of pH in either direction reduces the FMRFamide-gated current in AkFaNaC and the *Lymnaea* channel [26], indicating a complex action of H^+. Further experiments are required to elucidate the action of external H^+ on the channel function.

In the present study, we have characterized an *Aplysia* homologue of FaNaC. Functional expression of AkFaNaC confirms that the channel is a peptide-gated Na^+ channel. Although the FaNaCs are well conserved, there are some species specific portions especially in the large extracellular domain (see Fig. 1), probably related to some functional differences. Future

mutagenesis studies utilizing the structural differences among them will therefor give insights for the structure-function relationship of FaNaC including the puzzling actions of amiloride.

References

1. Adams CM, Snyder PM, WelshMJ (1999) Paradoxical stimulation of a DEG/ENaC channel by amiloride. J Biol Chem 274:15500–15504

2. Belkin KJ, Abrams TW (1993) FMRFamide produces biphasic modulation of the LFS motor neurons in the neural circuit of the siphon withdrawal reflex of *Aplysia* by activating Na^+ and K^+ currents. J Neurosci 13:5139–5152

3. Benos DJ, Stanton BA (1999) Functional domains within the degenerin/epithelial sodium channel (Deg/ENaC) superfamily of ion channels. J Physiol (Lond) 520:631–644

4. Coscoy S, de Weille JR, lingueglia E, Lazdunski M (1999) The pre-transmembrane 1 domain of acid-sensing ion channels participates in the ion pore. J Biol Chem 274:10129–10132

5. Coscoy S, Lingueglia E, Lazdunski M, Barbry P (1998) The Phe-Met-Arg-Phe-amide-activated sodium channel is a tetramer. J Biol Chem 273:8317–8322

6. Cottrell GA (1997) The first peptide-gated ion channel. J Exp Biol 200:2377–2386

7. Cottrell GA, Davis NW, Green KA (1984) Multiple actions of a molluscan cardioexcitatory neuropeptide and related peptides on identified *Helix* neurones. J Physiol (Lond) 356:315–333

8. Cottrell GA, Green KA, Davies NW (1990) The neuropeptide Phe-Met-Arg-Phe-NH_2 (FMRFamide) can activate a ligand-gated ion channel in *Helix* neurones. Pflügers Arch 416:612–614

9. Cottrell GA, Jeziorski MC, Green KA (2001) Location of a ligand recognition site of FMRFamide-gated Na^+ channel. FEBS Lett 489:71–74

10. Cropper EC, Brezina V, Vilim FS, Harish O, Price DA, Rosen S, Kupfermann I, Weiss KR (1994) FRF peptides in the arc neuromuscular system of *Aplysia*: Purification and physiological actions. J Neurophysiol 72:2181–2195

11. Ebberink RH, Price DA, Loenhout H, Doble KE, Riehm JP, Geraerts WP, Greenberg MJ (1987) The brain of *Lymnaea* contains a family of FMRFamide-like peptides. Peptides 8:515–522

12. Fujisawa Y, Ikeda T, Nomoto K, Yasuda-Kamatani Y, Kenny PTM, Muneoka Y (1992) The FMRFamide-related decapeptide of *Mytilus* contains a d-amino acid residue. Comp Biochem Physiol 102C:91–95

13. Green KA, Cottrell GA (2002) Activity modes and modulation of the peptide-gated Na^+ channel of *Helix* neurones. Pflügers Arch 443:813–821

14. Green KA, Falconer SWP, Cottrell GA (1994) The neuropeptide Phe-Met-Arg-Phe-NH_2 (FMRFamide) directly gates two ion channels in an identified *Helix* neurone. Pflügers Arch 428:232–240

15. Hille B (2001) Ionic channels of excitable membranes, 3rd edn. Sinauer Associates Inc, Sunderland

16. Immke DC, McCleskey EW (2003) Protons open acid-sensing ion channels by catalyzing relief of Ca^{2+} blockade. Neuron 37:75–84

17. Ishikawa T, Jiang C, Stutts MJ, Marunaka Y, Rotin D (2003) Regulation of the epithelial Na^+ channel by cytosolic ATP. J Biol Chem 278:38276–38286

18. Ismailov II, Kieber-Emmons T, Lin C, Berdiev BK, Shlyonsky VG, Patton HK, Fuller CM, Worrell R, Zuckerman JB, Sun W, Eaton DC, Benos DJ, Kleyman TR (1997) Identification of an amiloride binding domain within the α-subunit of the epithelial Na^+ channel. J Biol Chem 272:21075–21083

19. Jeziorski MC, Green KA, Sommerville J, Cottrell GA (2000) Cloning and expression of a FMRFamide-gated Na$^+$ channel from *Helisoma trivolvis* and comparison with the native neuronal channel. J Physiol (Lond) 526:13–25

20. Kellenberger S, Hoffmann-Pochon N, Gautschi I, Schneeberger E, and Schild L (1999) On the molecular basis of ion permeation in the epithelial Na$^+$ channel. J Gen Physiol 114:13–30

21. Kellenberger S, Schild L (2002) Epithelial sodium channel/degenerin family of ion channels; A variety of functions for shared structure. Physiol Rev 82:735–767

22. Lingueglia E, Champigny G, Lazdunski M, Barbry P (1995) Cloning of the amiloride sensitive FMRFamide peptide-gated sodium channel. Nature 378:730–733

23. McNicholas CM, Canessa CM (1997) Diversity of channels generated by different combinations of epithelial sodium channel subunits. J Gen Physiol 109:681–692

24. Palmer LG (1984) Voltage-dependent block by amiloride and other monovalent cations of apical Na channels in the toad urinary bladder. J Memb Biol 80:153–165

25. Paukert M, Babini E, Pusch M, Gründer S (2004) Identification of the Ca^{2+} blocking site of acid-sensing ion channel (ASIC) 1: Implications for channel gating. J Gen Physiol 124:383–394

26. Perry SJ, Straub WA, Schofield MG, Burke JF, Benjamin PR (2001) Neuronal expressoin of an FMRFamide-gated Na$^+$ channel and its modulation by acid pH. J Neurosci 21:5559–5567

27. Pfaffinger PJ, Furukawa Y, Zhao B, Dugan D, Kandel ER (1991) Cloning and expression of an *Aplysia* K$^+$ channel and comparison with native *Aplysia* K$^+$ currents. J Neurosci 11:918–927

28. Poet M, Tauc M, Lingueglia E, Cance P, Poujeol P, Lazdunski M, Counillon L (2001) Exploration of the pore structure of a peptide-gated Na$^+$ channel. EMBO J 20:5595–5602

29. Price DA, Lesser W, Lee TD, Doble KE, Greenberg MJ (1990) Seven FMRFamide-related and two SCP-related cardioactive peptides from *Helix*. J Exp Biol 154:421–437

30. Prosser CL (1973) Comparative animal physiology, 3rd edn. Saunders, Philadelphia

31. Rice P, Longden I, Bleasby A (2000) EMBOSS: the European molecular biology open software suite. Trends Genet 416:612–614

32. Ruben P, Johnson JW, Thompson S (1986) Analysis of FMRF-amide effects on *Aplysia* bursting neurons. J Neurosci 6:252–259

33. Schild L, Schneeberger E, Gautschi I, Firsov D (1997) Identification of amino acid residues in the α, β, γ subunits of the epithelial sodium channel (ENaC) involved in amiloride block and ion permeation. J Gen Physiol 109:15–26

34. Segal A, Awayda MS, Eggermont J, Driessche WV, Weber WM (2002) Influence of voltage and extracellular Na$^+$ on amiloride block and transport kinetics of rat epithelial Na$^+$ channel expressed in *Xenopus* oocytes. Pflügers Arch 443:882–891

35. Sheng S, Li J, McNulty KA, Kieber-Emmons T, Kleyman TR (2001) Epithelial sodium channel pore region: structure and role in gating. J Biol Chem 276:1326–1334

36. Shimizu Y, Kubo T, Furukawa Y (2002) Cumulative inactivation and the pore domain in the Kv1 channels. Pflügers Arch 443:720–730

37. Thompson JD, Higgins DG, Gibson TJ (1994) CLUSTAL W: improving the sensitivity of progressive multiple sequence alignment through sequence weighting, position-specific gap penalties and weight matrix choice. Nucleic Acids Res 22:4673–4680

38. Waldmann R, Champigny G, Lazdunski M (1995) Functional degenerin-containing chimeras identify residues essential for amiloride-sensitive Na$^+$ channel function. J Biol Chem 270:11735–11737

39. Weber WM (1999) Ion currents of *Xenopus laevis* oocytes: state of the art. Biochim Biophys Acta 1421:213–233

40. Woodhull AM (1973) Ionic blockage of sodium channels in nerve. J Gen Physiol 61:687–708

41. Zhainazarov AB, Cottrell GA (1998) Single-channel currents of a peptide-gated sodium channel expressed in *Xenopus* oocytes. J Physiol (Lond) 513:19–31